EEET ECOLOGICAL ENGINEERING & ENVIRONMENTAL TECHNOLOGY

Ecological Engineering & Environmental Technology 2023, 24(3), 79–89
https://doi.org/10.12912/27197050/157111
ISSN 2719–7050, License CC-BY 4.0

Received: 2022.11.03
Accepted: 2023.01.27
Published: 2023.02.25

Geophysical Study for the Recognition of the Water Resources of the Turonian Aquifer in the Eastern Part of the Boudnib Basin (Errachidia, Morocco)

Fadwa Laaraj[1*], Mohammed Benabdelhadi[1], Mohamed Chibout[2], Abderrahim Lahrach[1], Anasse Benslimane[2]

[1] Functional Ecology and Environmental Engineering Laboratory, Sciences & Technology Faculty, Sidi Mohamed Ben Abdellah University, Fez, Marocco

[2] Geodynamics and Natural Resources Laboratory, Faculy of Sciences Dhar Mahraz, Sidi Mohamed, Ben Abdellah University, Fez, Maracco

* Corresponding author's e-mail**:** fadwa.laaraj@gmail.com

ABSTRACT

The region of Boudnib is located in southeast Morocco and depends on the territorial region of Drâa-Tafilalet and the province of Errachidia. It has a water deficit due to the lack of rainfall in the region and the overexploitation of groundwater. 76 electrical drillings were drilled and correlated with borehole and seismic reflection data to understand and identify the structure and geometry of the deep aquifer to facilitate the selection of future boreholes and wells. After the interpretation of all data of vertical electrical sounding, we exploited it to make an interpretation of the results. Indeed, we have established an isohypse of the resistant roof maps also geoelectric sections representing the different electrical discontinuities present in the study area, their nature as well as the zones favorable to the exploitation of the Turonian aquifer waters.

Keywords: water resources, electrical sounding, seismic, resistivity, Boudnib basin, geometry.

INTRODUCTION

The Boudenib basin, covering an area of 15189 km², is located in the southeast of Morocco. It occupies a position of depression between two major structural areas: the Anti Atlas in the south and the High Atlas in the north and it is characterized by several aquifer systems with different water potentials.

The water resources in the region of Boudenib are in the process of destocking, especially those of the superficial aquifers. To reduce the effect of overexploitation of shallow aquifers, the use of water from deep aquifers remains a timely solution to fill the water deficit present in the region.

The reconstruction of the geometric configuration of the aquifer system in the Boudenib area can be improved, by integrating the data from the electrical drilling, by the identification of the resistivity, and thickness of each underground geological unit (Asfahani, 2007; Gouasmia et al., 2006; Zouhri et al., 2004; Toto et al., 2007; Guellala et al., 2009).

The region has been the subject of numerous geological and hydrogeological studies since 1930 (El Ouali, 2022; Roubil, 2022; Medina, 1994; Favre et al., 1991; Jossen and Filali, 1988; Makris et al.,1985; Adams A.E., 1979; Graf C., 1977; Chamayou and Richard, 1977; Michard, 1976; Du Dresnay, 1971–1975; Ambroggi R, 1963; Choubert and Faure Muret, 1960–1962; Margaret, 1954; Roch, 1950; Dubar and Despujols, 1939, 1943–49; Dagin, 1931). Several geophysical campaigns were realized in the Errachidia-Boudnib basin in the framework of groundwater research, Electrical prospecting began in the 1950s with small, scattered campaigns where it was possible to highlight the structural features of

the basin. The objective was to facilitate the location of exploratory drilling.

This work is to specify the geometric and structural architecture of the aquifers of the eastern part of the Boudenib basin, for reasonable management of these aquifers. to achieve this goal, we used data from electrical drilling in the study area correlated with hydraulic drilling data and seismic data.

These data were provided by the Agency of the Hydraulic Basin of Guir-Ziz-Rhéris, as for the interpretation of the electric drillings that were carried out within the company Africa Geo-Services.

General framework

The study area, located in southeastern Morocco, is limited to the north by the High Atlas, the west by the Wadi Guir, the south by the Hamadas of Guir, and the east by the palm Bouanane (Fig. 1).

The study area is part of the Cretaceous basin of Boudnib, and corresponds to a succession of plains and basins that separates the High Atlas in the north from the Anti-Atlas in the south and its extensions [Hindermayer, 1950]. Stratigraphically, the Plio-Quaternary covers the central and southern parts of the Boudnib region [Jossen and Filali, 1989]. It is formed of silts, sand, and alluvium with a variable thickness not exceeding 25 m. The continental Tertiary covers large areas. It extends eastward and southward to form the Hamada of Guir. It is represented by sandstones, conglomerates, clays, siltstones, and lacustrine limestones. It includes some gypsum and anhydrite. The Senonian outcrops to the north and south of Boudenib (Fig. 1). It is essentially constituted of relatively sandy or sandstone clay and even gypsiferous in places. The Cenomanian-Turonian outcrops in the northern part of the region and is made up of limestone formations with marly passages and become sandstone at their base.

The principal watercourse crossing the region of Boudenib is the Wadi Guir. Surface water inflows come mainly from the high-Atlasic basins in the form of violent and random floods [ABH-GZR,2011].

Hydrogeological, the aquifer is developed in the following formations:

- Carbonate and dolomitic formations of the Turonian age;
- Carbonate and dolomitic formations of the Conacian-Santonian base;
- The formations of the Senonian detrital sedimentation cone (Conglomerates and sandstones);
- The sandy formations of the Senonian.

MATERIALS AND METHODS

To meet the objectives of this study, we have exploited the data from all the drilling, electrical soundings, and seismic data that have been carried out and which have not been the subject of any hydrogeological synthesis to date.

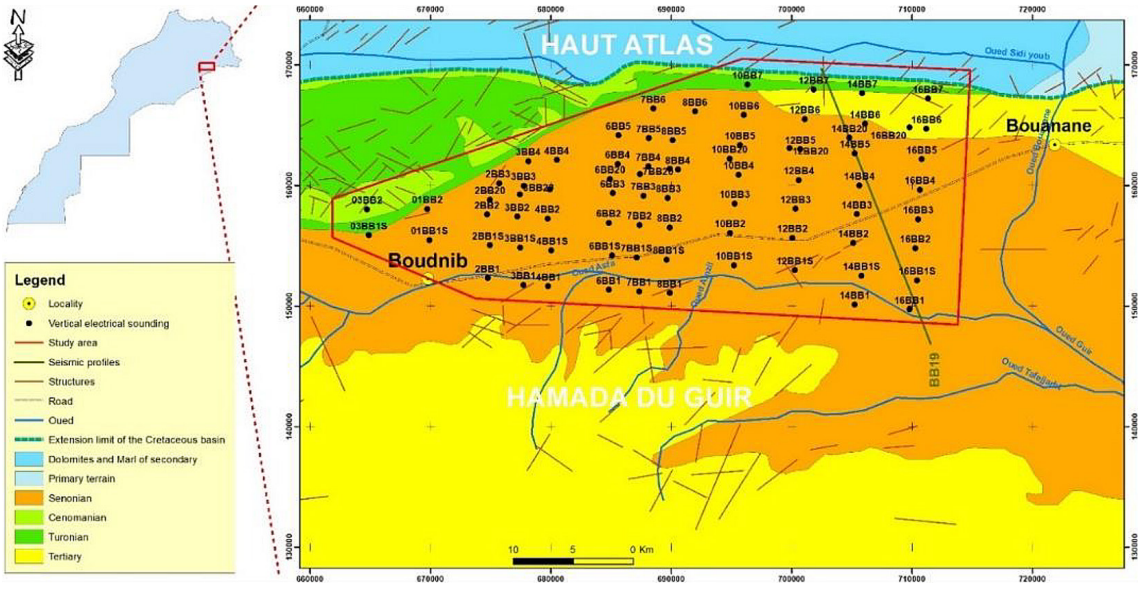

Fig. 1. Simplified geological sketch of the study area

In our study, we have taken up the surveys carried out by the Directorate of Water Research and Planning and the Bureau of Petroleum and Mining Research.

76 electrical soundings spread over an area of 810 m² were carried out (Fig. 1). These Schlumberger-type soundings are made with an AB line length between the emission electrodes of 10000 m.

Vertical electrical sounding (VES)

The electrical sounding method consists in establishing a vertical section of the ground resistivities under the central point of a quadrupole of electrodes. The potential difference ΔVMN between the measuring electrodes of the quadrupole is measured when a current IAB is injected between A and B. The apparent electrical resistivity obtained corresponds to the product of the measured electrical resistance by a coefficient depending on the position of the electrodes of the quadrupole (Fig. 2).

The device used is that of Schlumberger (A-MN-B). Data acquisition is performed with the ARESII resistivity meter.

Geo-electric field data was processed and interpreted after inversion by GeoStudi's Jean Louis Astier processing software (JLA plus), which objective is to determine the geo-electric parameters (thickness and resistivity) characterizing each layer, on the basis of the correlation with the lithological and hydrogeological data of the drilling available in the study area.

The results of this interpretation contributed to the construction of vertical electrical sounding (VES) models and geo-electric sections.

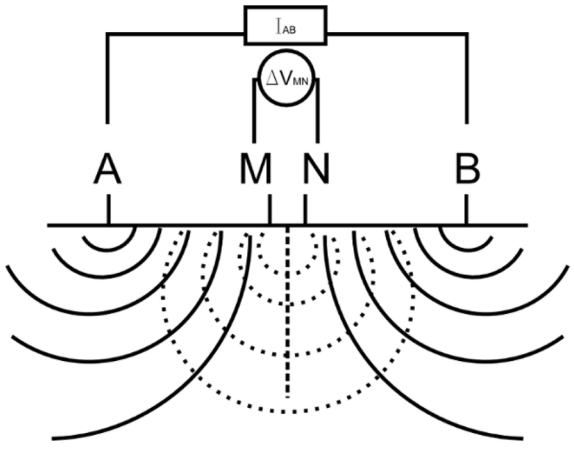

Fig. 2. Principle of the Schlumberger vertical electrical sounding (VES)

RESULTS AND DISCUSSION

The correlation between the electrical sounding data allowed us to differentiate three families of soundings (A, B, and C) (Fig. 2), each characterized by a different electrical response.

Family A

This family is characterized by the electrical sounding 3BB1S, The examination of its diagram shows the presence of an assembly represented by resistant and conductive layers (Ro, C), of a thickness of approximately 115 m (Fig. 3). According to the data from drillings F1, F2, F3, and F4 (Fig. 4), this ensemble corresponds to conglomerates and alternating sands and clays and could constitute a good aquifer.

The ensemble (Ro, C) overlies an intermediate level A1 with a resistivity of 47 Ω.m and a thickness of 205 m, under this cover (Ro, C, A1), we observe the presence of a resistant set (R2 + Rs) responsible for the rise of the curve (Fig. 3). This level is interspersed with a conductive C2 level (31 Ω·m – 195 m), whose presence is difficult to identify on the diagram, this level can be present in the R2 + Rs set by the effect of enrichment in conductive past (marl) which constitutes an anisotropic layer.

According to the results of seismic reflection and drilling (Fig. 4), the resistant level R2 (344 Ω·m – 230 m) corresponds to the sandstone and clay-limestone series of the Maastrichtian – Eocene. The conductive level C2 would correspond to the marly and gypsiferous series of the Santonian Campanian. The top of the resistant bedrock Rs would be the top of the Coniacian-Santonian and Turonian dolomitic limestones.

Family B

The curves of the electrical soundings 6BB3 and 7BB6 are plotted (Fig. 5) to highlight the plunge of the roof of the R2 + Rs resistance set from SEV 6BB3 to SEV 7BB6, and the important development of the C1 cover with a thickness that increases from 220 m (SEV 6BB3) to 330 m (SEV 7BB6). The diagram of the SEV 6BB3 shows in its lower part an electrical section similar to the one in the previous diagram (SEV 3BB1S). The conductive level C2 inserted in the resistive assembly

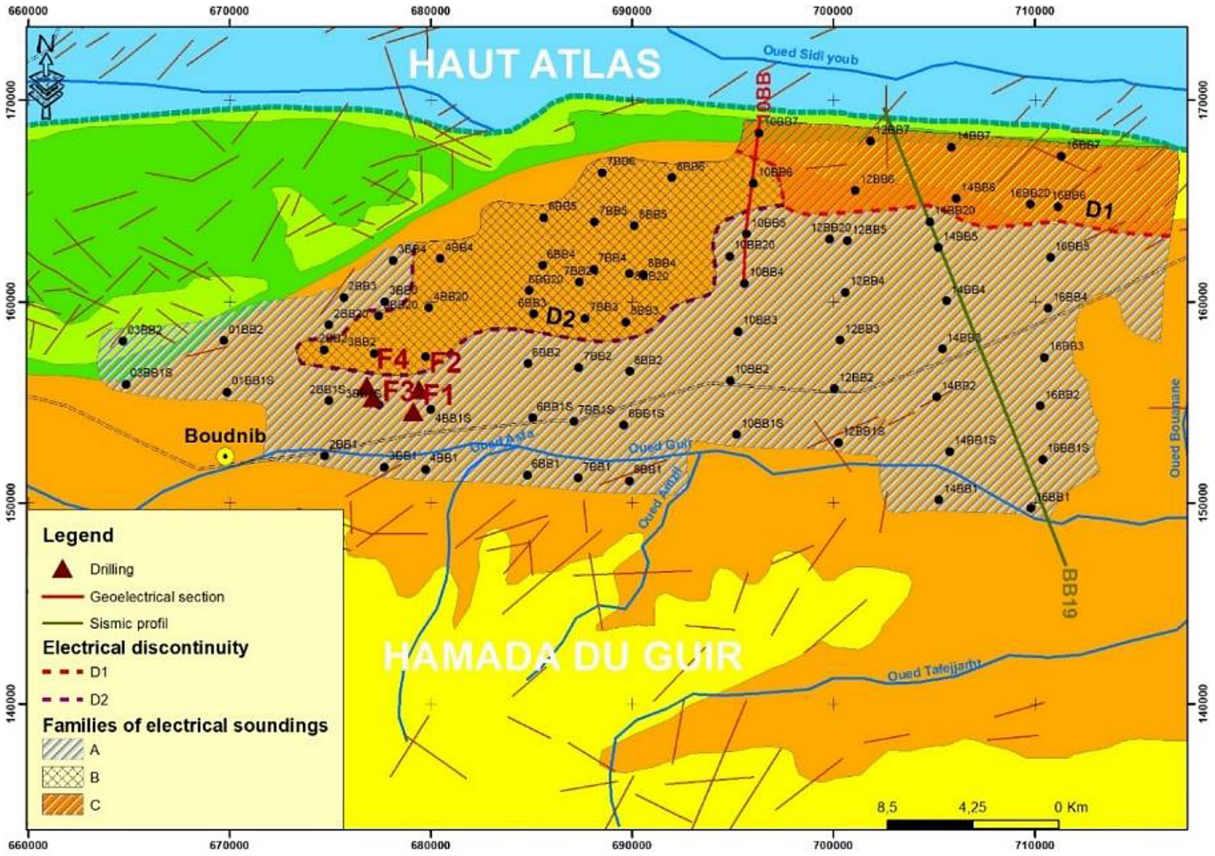

Fig. 3. Distribution of the families of electrical soundings

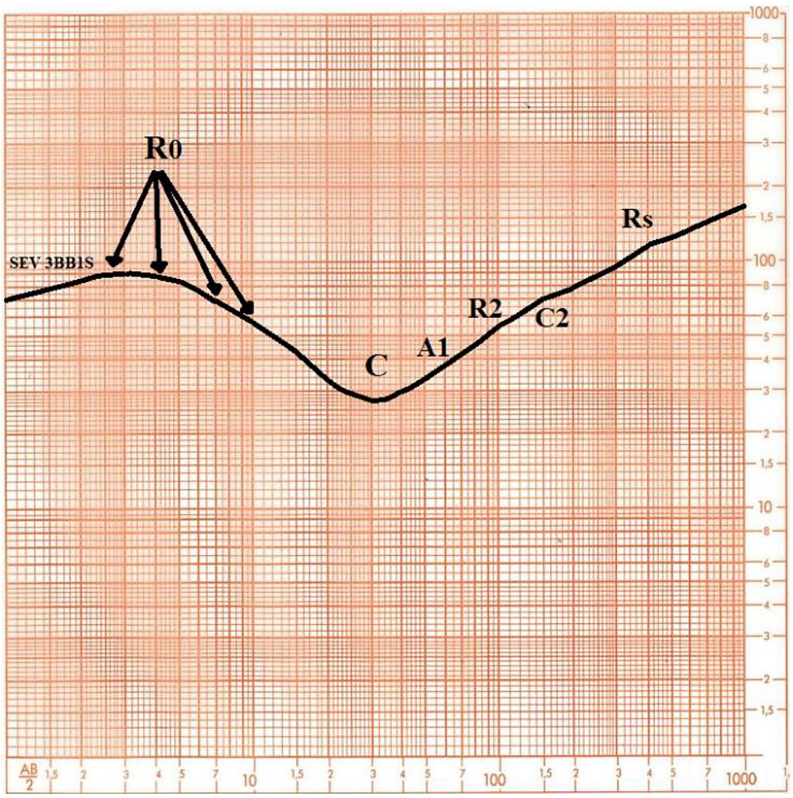

Fig. 4. Diagram of the electrical sounding 3BB1S.

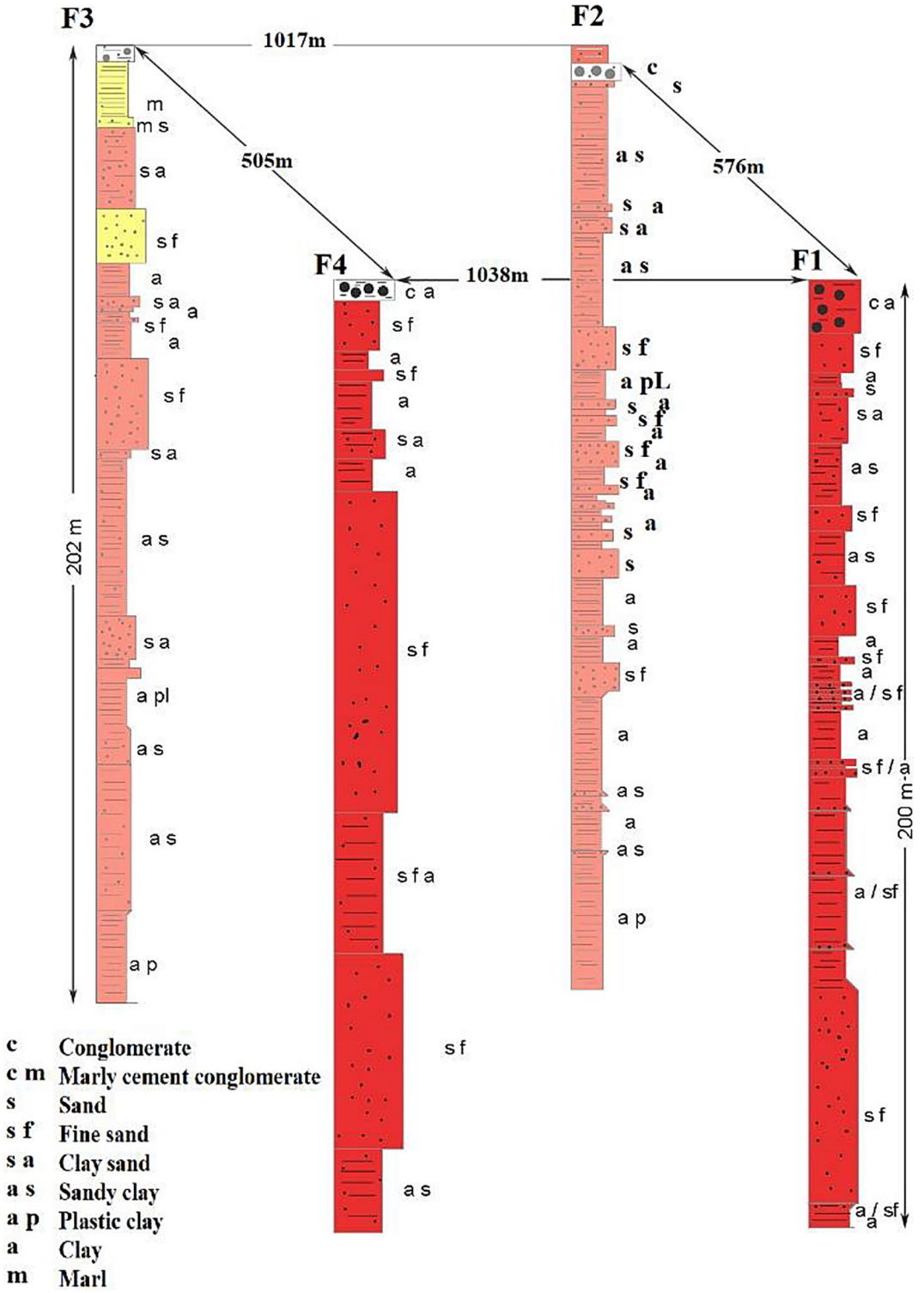

Fig. 5. Simplified lithological section of drillings F1, F2, F3, and F4

R2 + Rs with comparable physical characteristics, in this case, there is a change in the geoelectric behavior of the set (C, A1) of the SEV 3BB1S diagram which does not differ electrically from the set (D1, C1).

We notice an increase in the resistivity of the conductive level C1 from the South to the North of the electrical discontinuity D2. The roofs of the resistant levels R2 and Rs reach depths of 380 m and 755 m respectively.

Dans le diagramme du SEV 7BB6, aucune inflexion significative n'a été observée sur la montée de la courbe en raison de la faible valeur de la conductance longitudinale du conducteur C2 par rapport au conducteur C1. Then, we cannot estimate the depth of the resistor roof Rs.

Table 1. Resistivity and thickness of the electrical layers of SEV3BB1S

Layer (n)		Resistivity (Ω·m)	Thickness (m)	Depth (m)
R0	1 2 3 4	70 135 33 93	10 15 20 25	0 -10 -25 -45
C	5	12	115	-70
A1	6	47	205	-185
R2	7	344	230	-390
C2	8	31	195	-620
RS	9	210	Inf	-815

Table 2. Resistivity and thickness of the electrical layers of SEV6BB3

Layer (n)		Resistivity (Ω·m)	Thickness (m)	Depth (m)
R0	1 2 3	110 210 353	8 21 31	0 -8 -29
D1	4	108	100	-60
C1	5	30	220	-160
R2	6	410	195	-380
C2	7	50	180	-575
RS	8	270	Inf	-755

Table 3. Resistivity and thickness of the electrical layers of SEV7BB3

Layer (n)		Resistivity (Ω·m)	Thickness (m)	Depth (m)
R0	1 2 3	120 306 550	10 25 50	0 -10 -35
D1	4	120	140	-85
C1	5	24	330	-225
R2+RS	6	336	Inf	-555

Family C

This family of electrical soundings located to the NNE of the study area shows the presence of a 400 m-thick heterogeneous assemblage overlying a resistant R2' level (227 Ω·m – 420 m) (Fig. 6).

Below this level is a thick conductive level Cp (15 Ω·m – 1320 m) that overlies an infinitely resistant bedrock Rp whose roof reaches a depth of 2140 m.

The origin of the differences in the geoelectric properties of family C compared to those of A and B is the same. As one approaches the High Atlas (probably syn-orogenic cluse), the coarse detrital deposits are earlier, thus located below the discontinuity (Fig. 7), whereas further south, the H1 horizon approaches the base of the syn-orogenic detrital formations and thus the roof of the R2. a second factor intervenes and explains the origin of this difference: the ramp folds visible

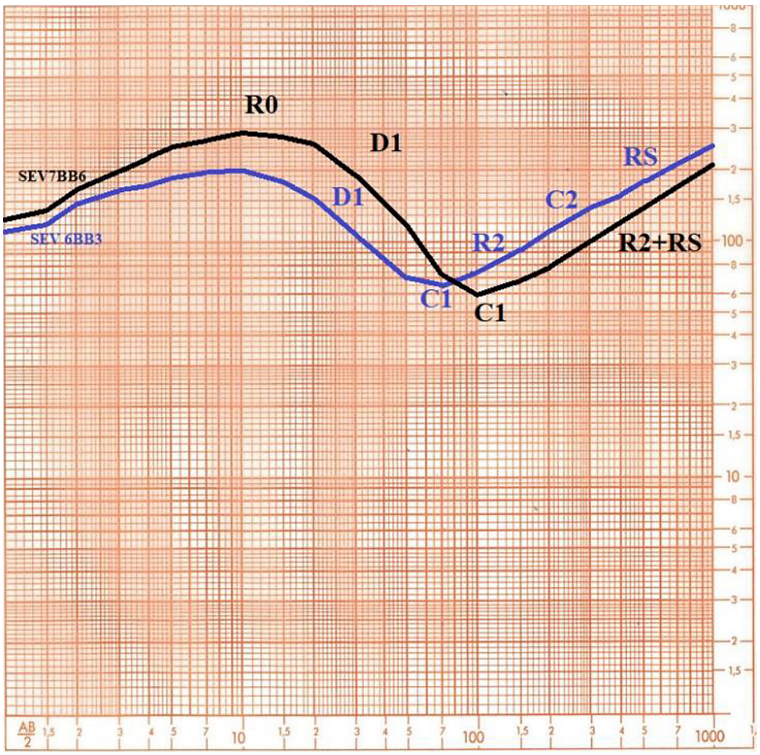

Fig. 6. Diagram of electrical soundings 7BB6 and 6BB3

in the North-East and affecting essentially the Tertiary conglomerates which outcrop in places (Fig. 7). The H1 horizon passes over the structure while the resistant bedrock roof R2 is located in a subhorizontal fracture zone. This has induced thickening of the Cp conductive level (separating some Tertiary deposits) and a deepening of the resistant R2 roof to the south of this zone. Thus, the geoelectric discontinuity D1 is of tectonic origin. Quant à l'horizon H2 (Fig. 7), il correspond au toit des formations Turoniennes.

The geoelectric section 10BB is chosen for a better comparison between geoelectric and seismic results, it crosses the three families of electrical sounding and the roofs of the orange Oligocene, yellow Santonian, and green Turonian horizons of the seismic profile.

From section 10BB we have observed a more or less variation of the terrain going from SEV 10BB4 to SEV 10BB7, this variation is well accentuated by the setting of a certain number of electrical discontinuities between SEV 10BB5 and 10BB6 it is the D2 discontinuity which is probably due to a fault, the second discontinuity D1 is located between the SEV 10BB6 and 10BB7 it is present according to the seismic (Fig. 7) to a ramp fold. North of this electrical discontinuity D1, the resistant bedrock Rs (Santonian and Turonian limestones) is probably eroded.

The electrical sounding family A is characterized by the presence of resistive level RS, the family B is characterized by the resistive level R2+Rs and the family C is characterized by the resistive level R'2.

Analysis of the isohypses maps

Following the quantitative interpretation of the electrical soundings, three isohypses maps are drawn, giving the appearance of the roofs of the resistant levels R2 + Rs, R2', and Rs. These maps are represented at a scale of 1/100.000 and with an equidistance of 20 m except for the isohypses map of the roof of the resistant level R2', where the equidistance is 50 m.

On the isohypse maps of the roof of resistors R2 + Rs and Rs the two electrical discontinuities D1 and D2 are plotted. The two electrical discontinuities D1 and D2 are plotted on the isohypses of the R2 + Rs and Rs resistors. On the isohypses of the roof of the resistant level R2', only the electrical discontinuity D1 has been traced, this is due to its absence in the other parts.

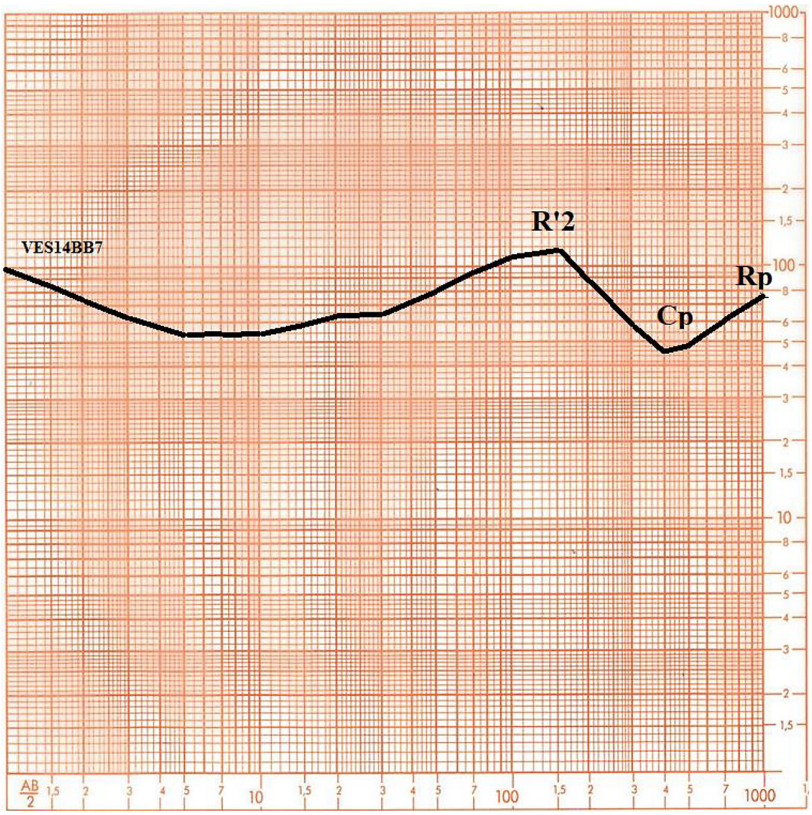

Fig. 7. Diagram of electrical sounding 14BB7

Isohypses map of the resistant ensemble R2 + Rs

Isohypses values vary considerably from 883 m (SEV 02BB2) for the highest point to 415 m (SEV 14BB20) for the lowest point. This map shows an area with a strong isohypses gradient located to the west and northwest and an area with a weak isohypses gradient to the east and south, It is divided into four zones, a high zone H characterized by a strong gradient of isohypses explaining the presence of an accentuated rise towards the northwest and west of the roof of the resistant R2 + Rs (Maastrichtian-Eocene). The highest point is located at SEV 2BB2 (883 m). This zone is limited by the electrical discontinuity D2, which would correspond to a flexure; A low zone S2 characterized by a strong gradient of isohypses, which explains a noticeable dip of the roof of the resistant R2 + Rs towards the north. The lowest point reaches a height of 305m at SEV 8BB6; A low zone of reduced extension S3 with a low gradient of isohypses is located in the vicinity of the city of Boudenib. The lowest point reaches a height of 540 m at the SEV 1BB1S; A low zone of vast extent S1 with a low gradient of isohypses which occupies the eastern part of the study area, its axis is substantially oriented SW-NE. The roof of the resistant R2 + Rs set dips to the NE to reach its lowest value of 415 m at SEV 14BB20.

Table 4. resistivity and thickness of the electrical layers of SEV14BB7

Layer (n)		Resistivity (Ω·m)	Thickness (m)	Depth (m)
R0	1	70	10	0
	2	135	15	-10
	3	33	20	-25
	4	93	25	-45
C	5	12	115	-70
A1	6	47	205	-185
R2	7	344	230	-390
C2	8	31	195	-620
RS	9	210	Inf	-815

North of the electrical discontinuity D1, another resistive level R2' (family C) is highlighted and presents physical characteristics that are different from those of the resistive level R2.

Isohypses map of the resistant roof R2'

This map (Fig. 10) was plotted only north of the electrical discontinuity D1. The isohypses vary considerably and range from 587 m (SEV 16BB6) for the highest point to 410 m (SEV 16BB7) for the lowest point. The analysis of this map highlights the presence of two depressions of a reasonably small extension at the level of soundings 12BB7 and 14BB7. These are separated by a high zone that reaches 550 m. The roof

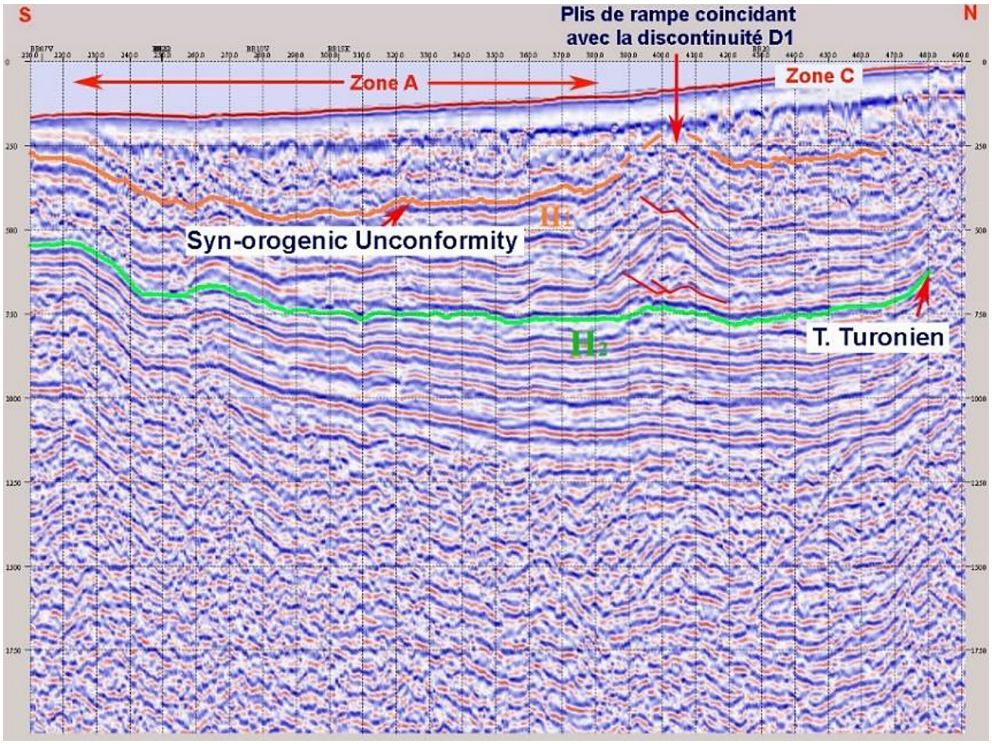

Fig. 8. Extract from seismic section BB19

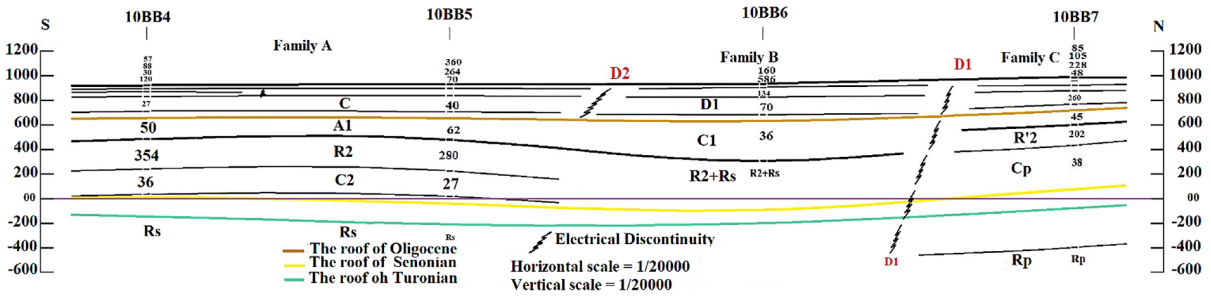

Fig. 9. Geoelectric section10BB

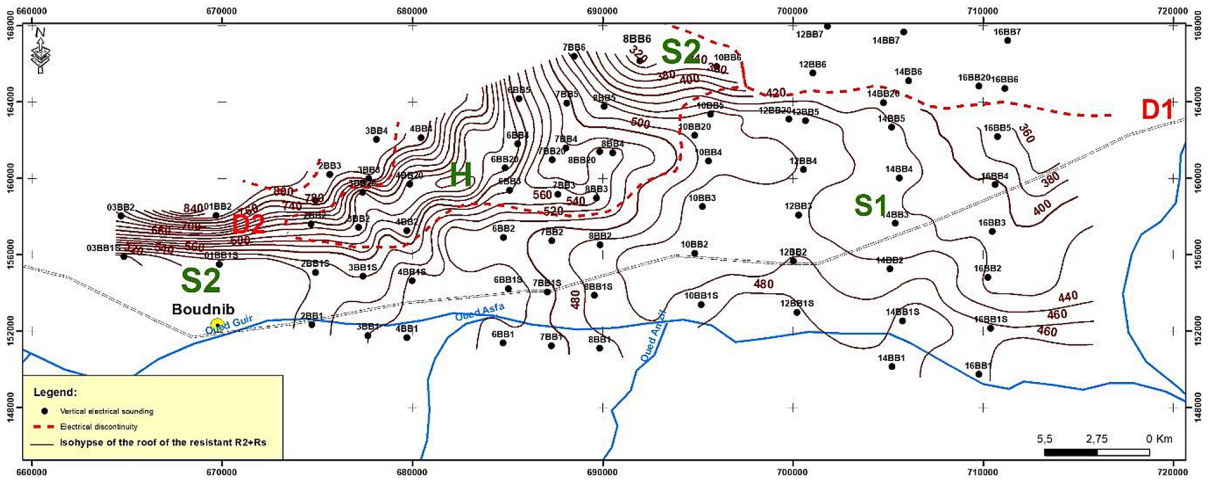

Fig. 10. Roof isohypses map of the resistant ensemble R2+Rs

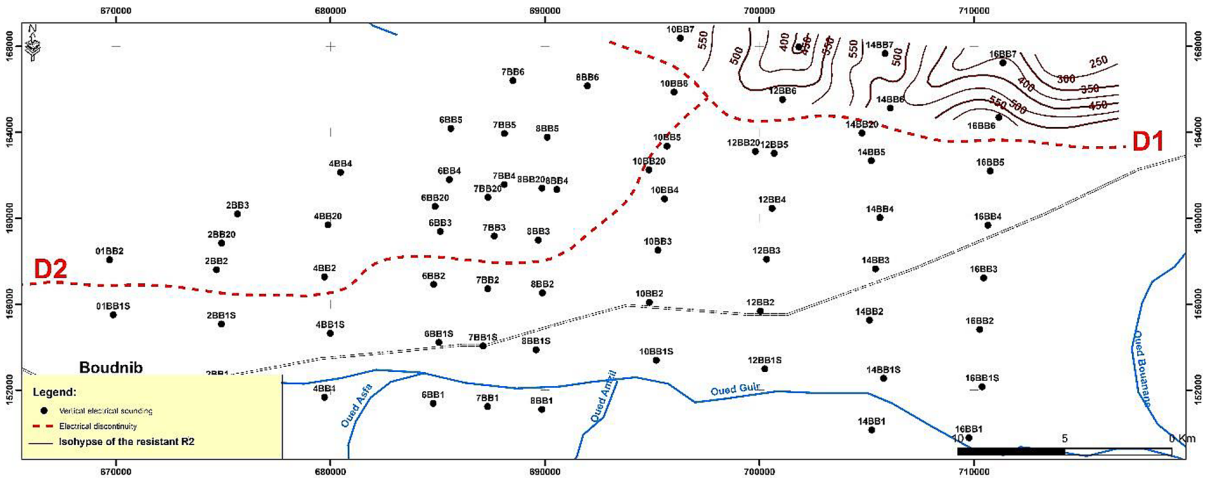

Fig. 11. Map of the isohypses of the roof of the resistant R2'.

of the resistant R2' rises towards the west at the level of SEV 10BB7 (583 m).

Isohypses map of the resistant ensemble Rs

The determination of the depth of the roof of the resistant Rs, especially towards the North (Fig. 11), at the edge of the electrical discontinuity D1, is conditioned by the thickness of the underlying conductor C2. its thickness remains uncertain because the conductive level C2 is sometimes, difficult to identify on the electrical sounding curves (Fig. 3). The nature of the C2 conductor (homogeneous isotropic layer or anisotropic layer) determines its physical characteristics.

The resistant bedrock map Rs (Santonian-Turonian) shows in its broad outlines a structural pattern similar to that of the resistant R2 + Rs roof isohypses map (Fig. 9), There is also the high zone H, where the highest point reaches a height

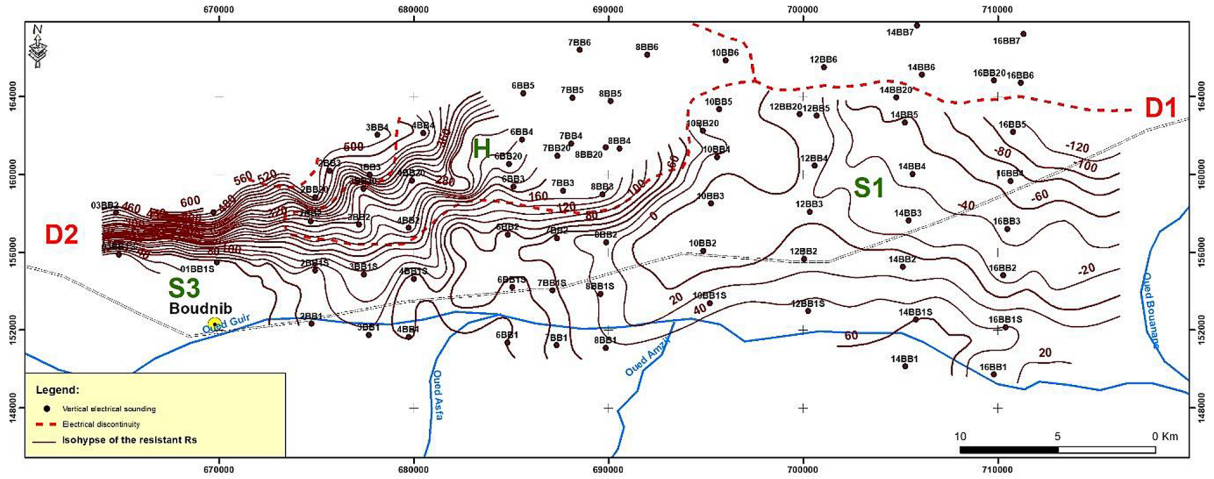

Fig. 12. Isohypses map of the resistant bedrock roof Rs.

of 618m at SEV 02BB2, and the two low zones S1 and S3, where the lowest points reach respectively -115 (SEV 16BB5) and 35 m (SEV 03BB1S).

CONCLUSIONS

The eastern part of the Boudenib Basin (Errachidia-Morocco), located in the south-east of Morocco, is essentially constituted by limestone and dolomitic limestone of Cenomano-Turonian, favoring an important hydrogeological reservoir that plays a decisive role both for the supply of drinking water in the region and for the irrigation of the agricultural lands of the basin.

This study reflects the interest of geophysical data for the knowledge of the geometry and structure of aquifers in the Boudenib Basin. The interpretation of these data has highlighted two electrical discontinuities D1 and D2, the first of which coincides with the heart of an anticline (ramp folds) that essentially affects the Tertiary and whose plane of detachment is located above the roof of the Turonian.

Examination of the isohypses maps of the roof of the resistant R2+Rs, Rs, and R'2 set revealed three depressions S1, S2, and S3 separated by the electrical discontinuities D1 and D2. At the foot of the High Atlas and south of the study area.

REFERENCES

1. ABH-GZR (Agence du Bassin Hydraulique de GUIR – GHRIS – ZIZ) 2007. Actualisation du Plan Directeur d'Aménagement Intégré des Ressources en Eau des Bassins de Guir – Ghris – Ziz et Maider.
2. ABH-GZR (Agence du Bassin Hydraulique de GUIR – GHRIS – ZIZ) 2011. Actualisation du plan directeur d'aménagement intégré des ressources en eau des bassins de Guir – Ziz – Rhéris et Maider. Rapport de synthèse.
3. Adams A.E. 1979. Sedimentary and palaeogeography of the western High Atlas, Morrocco during the middle and late Jurassic. Paleogeography, Palaeoclimatology, Palaeoecology, 28, 185–196.
4. El Ouali, A., Roubil, A., Lahrach, A., Mudry, J., El Ghali, T. et al. 2022. Isotopic characterization of rainwater for the development of a local meteoric water line in an arid climate: The case of the Wadi Ziz watershed (S-E Morocco). Water, MDPI, 14(5), 779.
5. Jossen, A., Filali, J. 1989. Le versant sud du bassin d'Errachidia : Synthèse stratigraphique et structurale ; Contribution à l'étude des aquifères profonds. Rapport de la Direction de la Recherche et de la Planification de l'Eau-Rabat.
6. Ambroggi R. 1963. Etude géologique du versant méridional du Haut Atlas Occidental et de la Plaine du Souss. N. Mém. Serv. Géol., 157; 321.
7. Chamayou J., Ruhard J.P. 1977. Sillon préafricain à l'est du Siroua: les bassins de Ouarzazate et de Errachidia (Ksar-es-Souk) Boudenib. In: Ressources en Eau du Maroc, tome 3, Domaines atlasique et sud-atlasique. Notes et Mémoires du Service géologique du Maroc, 231, 224–242.
8. Choubert, G., Faure-Muret, A. 1962. Evolution du domaine atlasique marocain depuis les temps paléozoiques. In: Livre à la Mémoire du Professeur Paul Fallot Mém. hors Sér., 1, 447– 527. Société géologique de France, Paris.
9. Dagin. 1931. le Crétacé de la vallée de l'Oued Ziz (Maroc du Sud Confins du Tafilelt).Bull. Soc. Géol. France, (5) t. I, fasc. 5–7, p. 537–545, 2 fig., 2 pl.
10. Dehbi, M. 1981. Permis Boudenib. Rapport d'interprétation. B.R.P.M. Division de l'exploration pétrolière, 12.

11. Dresnay, D. 1971–1975. Extension et développement des phénomènes récifaux jurassiques dans le domaine atlasique marocain, particulièrement au lias moyen. Bull. Soc. Géol. Fr., 7, 7(1–2), 46–56.
12. Dubar, D. 1949. Notice explicative de la carte geologique provisoire du Haut Atlas de Midelt au 1/200 000.
13. Toto, E.A., Kaabouben, F., Zouhri, L., Belarbi, M., Benammi, M., Hafid, M., Boutib, L. 2007. Geological evolution and structural style of the Palaeozoic Tafilalt sub-basin, eastern Anti-Atlas (Morocco, North Africa). Geological journal, 43(1), 59–73.
14. Graf C. 1977. Permis Boudenib. Rapport sur l'Interprétation des résultats de la Campagne sismique. Rapport du BRPM, 43.
15. Asfahani, J. 2007. Geoelectrical investigation for characterizing the hydrogeological conditions in semi-arid region in Khanasser valley, Syria. Journal of Arid Environments, 68(1), 31–52.
16. Hindermayer, J. 1950. Observations géologiques dans les Hamadas au Sud de Boudenib. Tome 3, Notes et Mémoires du Service Géologique du Maroc, 76, 105–139.
17. Jossen, J.A., Filali Moutei, J. 1988. Bassin d'Ouarzazate, synthèse stratigraphique et structurale. Contribution à l'étude des aquifères profonds – Projet PNUD – DRPE (Direction de la Recherche et de la planification de l'Eau) MOR /86/004- Exploration des eaux profondes. Rapport Inédit, 38.
18. Zouhri, L., Gorini, C., Deffontaines, B., Mania, J. 2004. Relationships between hydraulic conductivity distribution and synsedimentary faults, Rharb-Mamora basin, Morocco; Hydrogeological, geostatistical and modeling approaches. Hydrogeology Journal, 12, 591–600.
19. Makris, J., Demnati A., Klussmann, J. 1985. Deep seismic soudings im Morocco and a crust and upper mantle model deduced from seismic and gravity data. Annales Geophysicae, 3(3), 369–380.
20. Margat, J. 1954. Sédimentation actuelle par épandage des eaux de crue dans les palmeraies du Tafilalt (Maroc pré-saharien), dans Comptes-Rendus de la xe Assemblée Générale de l'Union de Géodésie et de Géophysique, Rome, 192–193.
21. Medina F. 1994. Evolution structurale du Haut Atlas Occidental et des régions voisines du Trias à l'Actuel, dans le cadre de l'ouverture de l'Atlantique Central et de la collision Afrique-Europe. Thèse Univ. Mohammed V, Rabat, 272.
22. Michard A. 1976. Eléments de géologie marocaine. Notes et Mém. Serv. Carte géol. Maroc, 252, 408.
23. Mouez G. 2006. Prospection géoélectrique pour l'étude de l'aquifère thermal des calcaires récifaux, Hmeïma–Boujabeur (Centre ouest de la Tunisie) Geoelectrical prospecting for studying the thermal aquifer of reef limestone, Hmeïma–Boujabeur (central–western Tunisia). Comptes Rendus Geoscience, 338(16), 1219–1227.
24. Guellala, R., Inoubli, M.H., Amri, F. 2008. Nouveaux éléments sur la structure de l'aquifère superficiel de Ghardimaou (Tunisie): contribution de la géophysique électrique / New elements on the structure of the Ghardimaou superficial aquifer (Tunisia): electrical geophysics results. Hydrological Sciences Journal, 54(5), 974–983.
25. Roubil, A., El Ouali, A., Bülbül, A., Lahrach, A., Mudry, J., Mamouch, Y., Essahlaoui, A., El Hmaidi, A., El Ouali, A. 2022.Groundwater Hydrochemical and Isotopic Evolution from High Atlas Jurassic Limestones to Errachidia Cretaceous Basin (Southeastern Morocco). Water, 2022, 14.
26. Roth, E. 1950. Histoire stratigraphique du Maroc. Notes et M&noires du Service Geologique du Maroc, 80, 440.